Check for updates

RESEARCH ARTICLE

NANO · MICRO small
www.small-journal.com

Amplifying Touch Using 3D ZnO Tetrapods for Tactile and Haptic Intelligence

*Parth Pandit, Mahesh Y. Chougale, Deepak Dubal, Yogendra Kumar Mishra, Graham Kerr, and Ajay K. Pandey**

Advances in tactile and haptic intelligence are driven by development of advanced funtional materials capable of translating subtle physical interactions into precise electrical signals. This study presents an innovative approach to enhancing touch sensitivity by incorporating 3D Zinc Oxide (ZnO) tetrapods into a piezoelectric polymer matrix. The distinctive 3D architecture of the ZnO tetrapods significantly improves the mechanical-to-electrical conversion efficiency, thereby amplifying the material's ability to detect fine tactile forces. We optimized the loading of ZnO tetrapods within a Polyvinylidene fluoride (PVDF) matrix, resulting in a highly responsive composite material for tactile sensing. It exhibited exceptional performance in detecting minute pressure variations, with just 4 wt.% tetrapods in the polymer matrix. Output voltage and current of the composite matrix increased from 4 V, 0.5µA to 19 V, 2.5µA respectively when the concentration of the ZnO tetrapods is gradually increased from 0–4 wt.% and decreased with further increase in tetrapod concentration. Comprehensive analysis and applications of this piezoelectrical materialconfirmed its robustness across a range of pressure conditions. The amplification of touch sensitivity and signal responsiveness underscores the potential of 3D ZnO tetrapods for tactile and haptic technologies.

1. Introduction

In theera of digital revolution underlined by the internet of things (IoTs) and artificial intelligence, technologies that capture human-machine interaction or machine to machine interaction are becoming prominent.[1] The rapid rise of wearable electronics in application domains such as e-skins, soft robotics, intelligent clothing, healthcare devices, energy harvesting, and storage systems is defining technological prowess of advanced sensors in almost every aspect of modern technology.[2] For instance, e-skins can be used in human-robot interaction for tactile perception, which then expands to assistive devices and rehabilitation training systems.[3] Moreover, in pixelated form such devices can differentiate multiple stimuli simultaneously for tactile perception. Their mechanical flexibility, biocompatibility, and energy harvesting ability make them a perfect core of future electronics innovations [4] However, mechanical flexibility if not optimised for function, makes them prone to local material delamination or cracking under repeated tension and strain, compromising their reliability and longevity.[5] Additionally, the miniaturized and thin form factor of wearable electronics often puts desing limits on free space required for housing sizeable batteries. Such constraints on battery capacity necessitates frequent recharging, which significantly hampers its core function and overall user experience.[6] To address these issues, one can either enhance the battery performance by designing low-power consuming devices or create a self-powered mode by energy harvesting on the fly.[7] To address these constraints, self-powered sensory systems, capable of harnessing energy from mechanical stimuli to power electronic devices while simultaneously responding to various external stimuli, has garnered significant attention, and are particularly desired for IoTs designed to meet Industry 5.0 goals.[6,8]

P. Pandit, A. K. Pandey
School of Electrical Engineering and Robotics
Queensland University of Technology
Brisbane, QLD 4000, Australia
E-mail: a2.pandey@qut.edu.au

The ORCID identification number(s) for the author(s) of this article can be found under https://doi.org/10.1002/smll.202408414

© 2025 The Author(s). Small published by Wiley-VCH GmbH. This is an open access article under the terms of the Creative Commons Attribution-NonCommercial-NoDerivs License, which permits use and distribution in any medium, provided the original work is properly cited, the use is non-commercial and no modifications or adaptations are made.

DOI: 10.1002/smll.202408414

M. Y. Chougale, D. Dubal
Centre for Materials Science, School of Chemistry and Physics
Queensland University of Technology
Brisbane, QLD 4000, Australia

Y. K. Mishra
Smart Materials
Mads Clausen Institute
University of Southern Denmark
Alsion 2, Sønderborg 6400, Denmark

G. Kerr
Movement Neuroscience Group
School of Exercise and Nutrition Sciences
Queensland University of Technology
Brisbane, QLD 4059, Australia

Among others, the piezoelectric nanogenerators (PENGs) are promising candidates for converting mechanical movements such as tactile stimuli,[9] wind,[10] drops,[11] ocean waves,[12] into electrical energy by surface charging (triboelectric) mechanism.[6] The PENGs have unique advantages to be self-powered and responsive to dynamic stress with high sensitivity, high accuracy, at enhanced piezoelectric coefficient.[13] Material-based PENG investigations have undergone a lot of progress in gases, pressure, and temperature sensing. The state of art piezoelectric sensors are built out of conductive materials, substrates, polymers, and circuits. Over the past few years, many piezoelectric sensors have been reported with energy harvesting applications such as barium titanate ($BaTiO_3$),[14] aluminum nitride (AlN)[15] and lead zirconate titanate (PZT)[16] including many others. For advanced functional outreach of such devices, individual materials cannot satisfy the desired needs. Often the required functionalities are achieved by designing the multicomponent material by combining two or more materials in composite form. For example, the polymer nanocomposites out of fibrous $BaTiO_3$ reinforced in poly(vinylidene fluoride) (PVDF) nanocomposite is reported as a capable material for transducer applications.[17] The poly(dimethyl-siloxane) impregnated with multiwalled carbon tubes nanocomposite has been utilized as flexible pressure sensors.[18] The conventionally used PZT based sensors lack the desired softness and flexibility and additionally, PZT is toxic in nature which is a big environmental concern. As an alternative, the zinc oxide (ZnO) nanostructures incorporated cellulose fiber-based polymer nanocomposite material is reported as a good candidate for strain sensing.[19] In the same line of thought, the electrospun piezoelectric nanocomposite fibers fabricated from ZnO nanorods and PVDF polymer have demonstrated a great strain sensing ability and are already being used for real-time sensing of internal micro pressure in arteries.[20]

As an inorganic material, ZnOis a very versatile candidate for nanostructuring because of its hexagonal-wurtzite crystal structure (*c*-axis as fastest growth axis). The non-centrosymmetric crystal structure in wurtzite nicely facilitates the ZnO nano-microstructures with piezoelectric properties. The Zn^{2+} and O^{2-} terminated polar surfaces along the *c*-axis make the surface of ZnO nanostructures to be functionally very active which is relevant for many sensing applications.[21] ZnO exhibits a wide bandgap of 3.37 eV with an exciton binding energy of 60meV and almost any imaginary nanostructure can be grown easily which gives rise to various applications.[22] With their high surface-to-volume (S/V) ratio, typical n-type conductivity, UV-sensitive bandgap, and terminated polar surfaces, the ZnO micro and nanostructures offer significant promises for nanoelectronics and sensor development. Their active surface offers significant interaction area with polymers and hence these micro and nanostructures have been used as novel filler candidates in the polymers.[23] The ZnO micro and nanostructures with various ZnO morphologies have been synthesized and used as novel inorganic fillers in polymers to fabricate advanced piezoelectric nanocomposites.[24] The ZnO morphologies include nanoparticles, nanorods, nanowires, nanotubes, nanopillars, nanoflowers, etc. in the polymer as piezoelectric nanocomposites.[25,26] The 1D morphology, i.e., nanorod and nanowire of ZnO is the most explored system with respect to piezoelectric performance[25] and they have been used as filler component to enhance the overall piezoelectric response of nanocomposites.[27] While using 1D ZnO nanostructures as fillers in the polymers, uniform dispersion and alignments of fillers inside the composite is a big challenge. In a non-homogeneous filler distributed composite, they align differently which impacts the overall piezoelectric performance of the composite. The role of appropriate filler becomes very crucial for improving the piezoelectric performance of the composite.[28] There exists a novel 3D geometry of ZnO micro- and nanostructure, in the form of tetrapod which offers excellent avenues to upgrade the piezoelectric performance of the composites, if used as filler. The ZNO tetrapods are built out of four 1D wurtzite micro-nanorods in the form of 3D morphology where all the arms are interconnected via a central crystalline core at an angle of ≈110° with respect to each other.[29] The tetrapod geometry offers unique advantage in the sense, that irrespective of how they are handled, they enquivocally form a self-assembled highly porous 3D architecture. Their arms prohibit their agglomerations in the polymers and hence a well-dispersed composite system can be designed. Due to this feature, these ZnO tetrapods have already been utilized in many composite engineering applications.[24] Since ZnO tetrapods are built out of four wurtzite arms, they exhibit interesting piezoelectric responses under the impact of pressure/force. The force on one arm bends the other three arms in other directions accumulating an overall piezoelectric response.[30] Additionally, under pressure, the strained central core improves the carrier density, thereby improving the electrical conductivity.[31] These tetrapods can be novel piezoelectric filler components to improve the overall piezoelectric performance of a composite by embedding them in the appropriate polymer matrix. These ZnO tetrapods are extremely eco-friendly/biocompatible and also can be produced in large quantities by very simple methods. In short, ZnO tetrapods are unique and special due to their 3D morphology and have four needle or rod-shaped wurtzite-structured legs or arms.[29]

While PVDF, a semi-crystalline polymeric-based piezoelectric material, has gained lots of interest for practical piezoelectric applications due to its good flexibility and biocompatibility.[32] Although, PVDF exhibits five different crystalline polymorphs based on the polymer chain structure: α, β, γ, δ, and ϵ. The polar β phase was reported to exhibit the highest piezoelectricity due to the very large dipole moment in the structure.[33] Inspired by the significant abilities of PVDF polymer, we aimed to use it as the host matrix material for ZnO tetrapods.

In this work, we present the design, fabrication and performance of a highly sensitive and flexible electronic skin (e-skin) leveraging piezoelectricity through compositional engineering of PVDF and ZnO tetrapods. By employing a straightforward and cost-effective solution casting technique, we have significantly enhanced the piezoelectric properties by achieving performance levels nearly comparable to those of the more commonly used piezoelectric materials. This enhancement is attributed to the optimal ratio and compositional engineering with inorganic ZnO tetrapods fillers, which effectively induce spontaneous polarization in PVDF. Our work offers a low-cost, high-performance piezoelectric nanogenerator (PENG) that serves as a highly flexible and intelligent e-skin, with potential applications in advanced healthcare and other cutting-edge technologies.

© 2025 The Author(s). Small published by Wiley-VCH GmbH

16136829, 0, Downloaded from https://onlinelibrary.wiley.com/doi/10.1002/smll.202408414 by Zaffar Shaikh - Benazir Bhutto Shaheed , Wiley Online Library on [15/04/2025]. See the Terms and Conditions (https://onlinelibrary.wiley.com/terms-and-conditions) on Wiley Online Library for rules of use; OA articles are governed by the applicable Creative Commons License

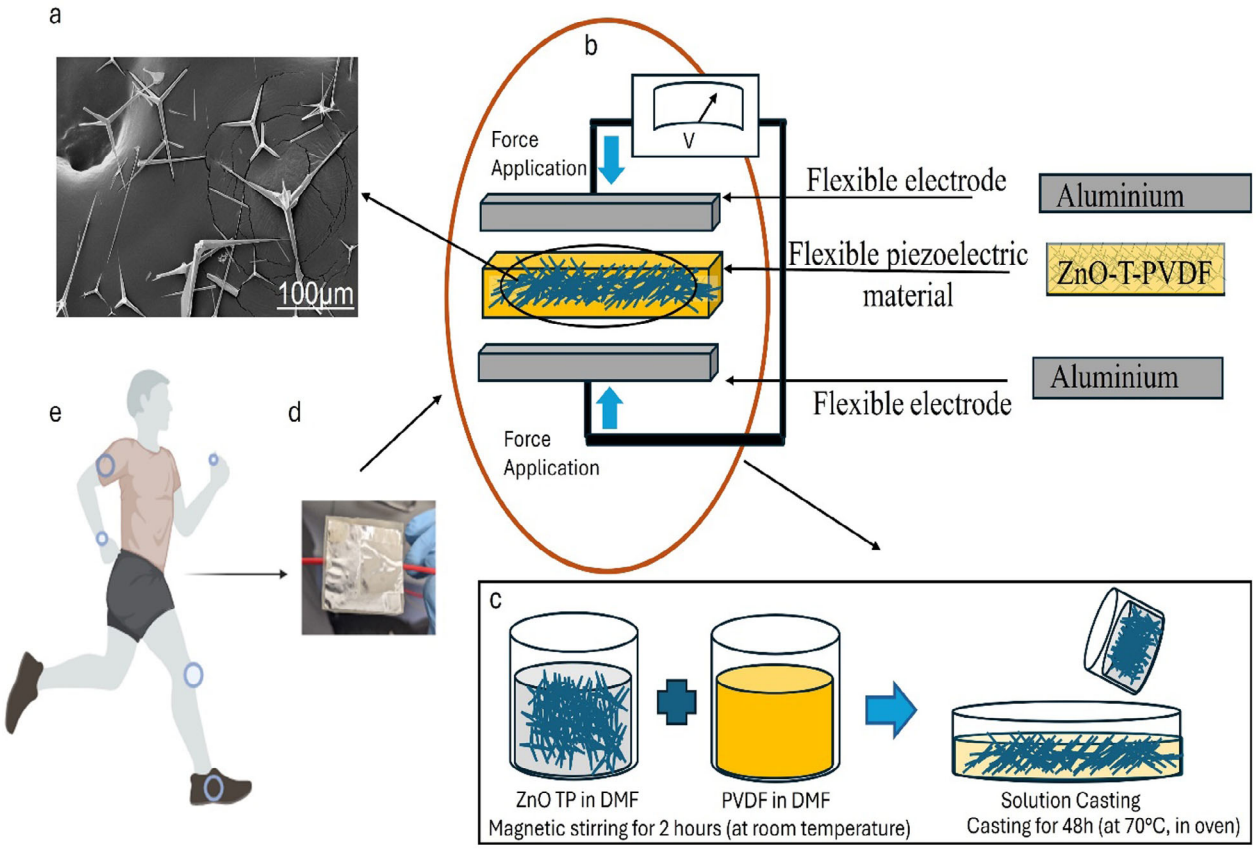

Figure 1. Schematic illustration of fabrication ZnO tetrapod -PVDF nanocomposite PENG a) SEM image of bare zinc oxide tetrapods showing its distinctive 3D morphology with the central crystalline core. b) Symmetric piezoelectric nanogenerator with ZnO tetrapod-PVDF composite and aluminum electrodes. c) Synthesis of ZnO tetrapod-:PVDF films using solution casting method. d) Digital photograph of the packaged device for sensing pressure. e) Human motion monitoring using fabricated piezoelectric nanocomposite.

2. Experimental Section

2.1. Material Details

Poly(vinylidene fluoride) pellets (PVDF, MW ≈275000 g mol^{-1}) and *N*, *N*-dimethylformamide (DMF) were purchased from Sigma–Aldrich. The PDMS used was obtained from Dow Corning. The ZnO tetrapod powder was synthesized in house and used for further analysis.

2.2. Synthesis of ZnO-T Micro and Nanostructures

The ZnO tetrapod micro and nanostructures were synthesized by a newly developed simple and novel flame transport synthesis (FTS) approach.[34] All chemicals were used without further purification and treatment. For the ZnO tetrapod synthesis, a ceramic crucible is filled with precursor material which was a mixture of zinc microparticle powder and polyvinyl butyral (PVB) in the weight ratio of 1:2. The Zn particles were precursor however, PVB's was just sacrificial to generate the flame and help in converting the Zn microparticles into atomic vapor.[35] The ceramic crucible filled with precursor mixture was inserted into a simple muffle furnace for the growth process at 900 °C. After a process of 30 min at 900 °C, the heating was turned down and the furnace was left to cool down naturally. After the process, the crucible was filled with white snowflakes like ZnO micro and nanoscale tetrapods which were carefully harvested and used for desired purposes. These tetrapods were grown in a dedicated furnace (only ZnO growth) so the obtained structures were pure with respect to any external impurity. However, due to the high-temperature thermodynamic process, these tetrapods exhibit intrinsic defects which include twin/grain boundaries and also a lot of surface structures (nanostairs, wrinkles, ripples, etc.) which in turn increase the overall surface contribution and hence high surface activity.[35]

2.3. Preparation of Zinc Oxide Tetrapod Incorporated PVDF Films

PVDF (3 g) was weighed and added to 50 mL of DMF. The formation was stirred for 2 h at 60 °C to obtain a clear solution. On the other hand, five glass vials were taken and 5 mL of DMF was added to each one. Different mass loading of synthesized ZnO tetrapods as 0.5%, 1%, 2%, 4%, and 6% was added to five vails, and the sixth was marked as bare. These ZnO tetrapods inDMF solutions were sonicated for 10 mins to obtain a uniform dispersion. 5 mL of PVDF-DMF were added to all the six vials having ZnO tetrapods dispersed in DMF and set for strong stirring for

© 2025 The Author(s). Small published by Wiley-VCH GmbH

16136829, 0, Downloaded from https://onlinelibrary.wiley.com/doi/10.1002/smll.202408414 by Zaffar Shaikh - Benazir Bhutto Shaheed , Wiley Online Library on [15/04/2025]. See the Terms and Conditions (https://onlinelibrary.wiley.com/terms-and-conditions) on Wiley Online Library for rules of use; OA articles are governed by the applicable Creative Commons License

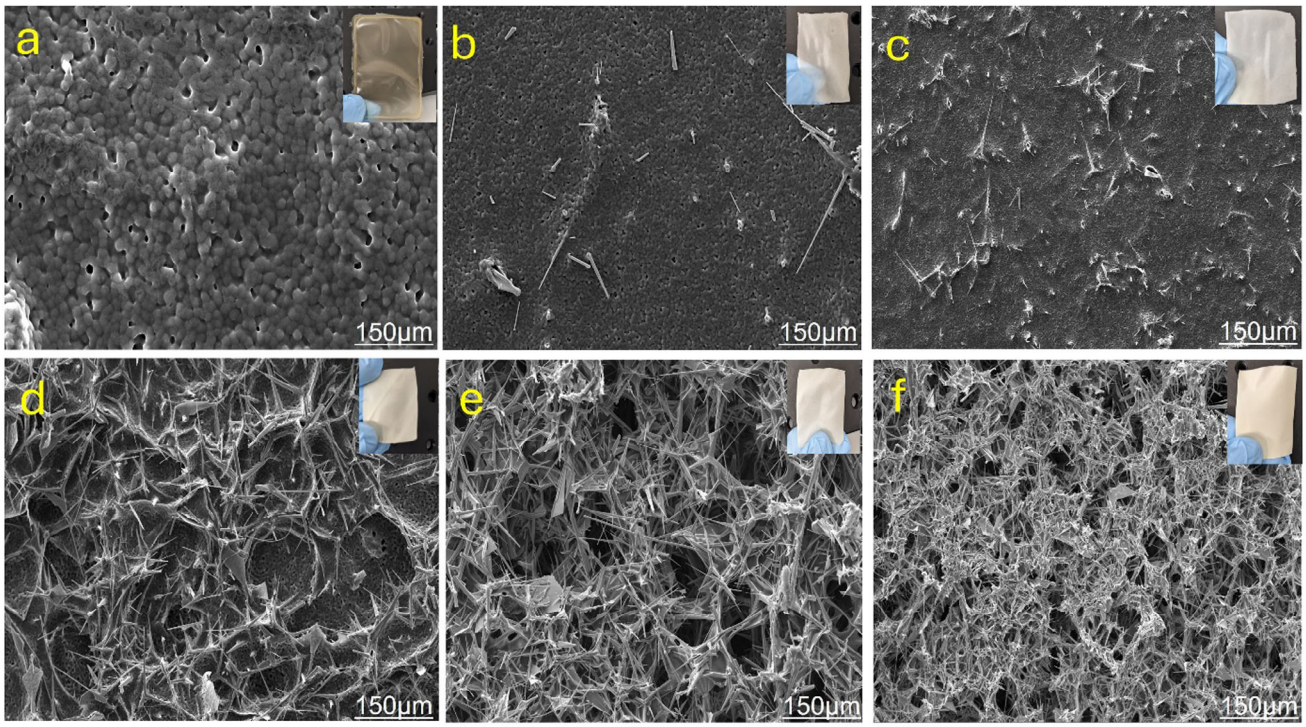

Figure 2. a–f) Top-down surface SEM images of pure PVDF with 150 μm scale a) and comparison with ZnO-Ts embedded within the PVDF matrix of the same scale. The addition of ZnO-Ts to pure PVDF results in changes in the polymer matrix leading to the distribution of tetrapods in the matrix ranging from b) 0.5%, c),1% d) 2%, e) 4%, f) 6%. Inset the photographs of fabricated composite films.

6 h at room temperature to obtain uniform dispersion. The overall mixed solutions were poured into glass molds (10 cm × 10 cm) for casting, followed by drying in a hot air oven for 48 h at 70 °C. The dried films were peeled from the substrates and cut into standard size of (3 cm × 2 cm) after the curing procedure and used for further analysis.

2.4. Fabrication of Piezoelectric Nanogenerator

The piezoelectric energy harvesting device was fabricated by integrating a functional ZnOtetrapod /PVDF composite film between two electrode layers. Commercial aluminum adhesive tapes served as the electrodes; their conductive sides were adhered to the surfaces of the composite film, while the adhesive sides were affixed to polydimethylsiloxane (PDMS) layers. PDMS, a widely used packaging material, provides structural integrity to the device and shields it from external damage. The PDMS layers encapsulate the top and bottom electrodes, creating a robust sandwich configuration. The schematic diagram (**Figure 1**) illustrates the detailed fabrication process of the nanocomposite film and the energy harvesting device.

2.5. Body Worn Device Fabrication

The process for fabricating body-worn sensors was quite like the one previously described for PENG used as an energy harvester and nonhuman contact sensor. To secure the device on the human body during motion recognition tests, polyimide tape was used for attachment and reinforcement.

3. Results and Discussion

3.1. Structural Studies

The distribution of ZnO tetrapods in PVDF matrix was determined by SEM results. Figure 1a represents bare ZnO tetrapods and **Figure 2**a–f is its comparison with ZnO tetrapod doped films in the PVDF polymer matrix. From the SEM results, we can conclude that pure PVDF films without any impregnated ZnO tetrapod sample have an amorphous polymeric structure with a randomly distributed polymer chain cluster. Adding 0.5% tetrapods in the PVDF matrix results in tetrapods scarcely distributed in the PVDF matrix. When the tetrapod concentration was increased to 1% and 2%, the higher concentration of ZnO tetrapods was seen in the polymer matrix and still it appeared to be distributed uniformly. When the concentration was increased to 4%, we can see agglomeration of particles started to dominate as shown in Figure 2e. At a concentration higher than this which is 6% (Figure 2f) ZnO tetrapods dominate the matrix while also decreasing the piezoelectric performance as per the output voltage measurement, which will be discussed in the section on energy harvesting studies. The ZnO- tetrpod/PVDF composite films are shown in the photographs (Figure 2f). A slight variation in film thickness was observed as ZnO tetrapod doping increased. However, the thickness does not affect piezo perfor-

© 2025 The Author(s). Small published by Wiley-VCH GmbH

16136829, 0, Downloaded from https://onlinelibrary.wiley.com/doi/10.1002/smll.202408414 by Zaffar Shaikh - Benazir Bhutto Shaheed , Wiley Online Library on [15/04/2025]. See the Terms and Conditions (https://onlinelibrary.wiley.com/terms-and-conditions) on Wiley Online Library for rules of use; OA articles are governed by the applicable Creative Commons License

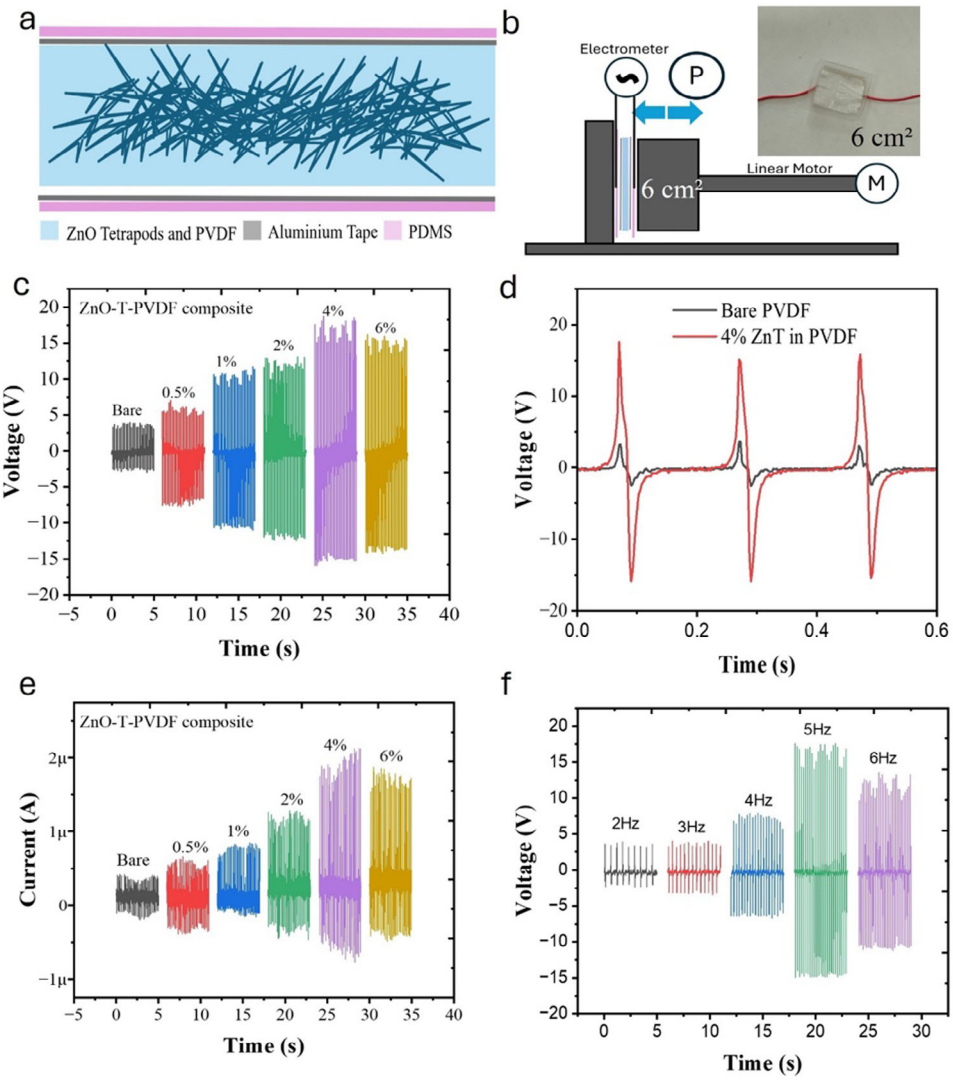

Figure 3. PENG device measurement results. a)The device structure of the piezoelectric nanogenerator. b) Schematic diagram of the measuring mode used for sensing and photograph of fabricated nanogenerator device. The P denotes pressure applied with different frequencies via a linear motor. c) Output circuit voltage variation as a function of the ZnO-Ts concentration in the PVDF matrix. The highest output voltage was obtained for 4% ZnO-Ts-doped samples. d) Comparison of voltage output of pristine PVDF and 4% ZnO-Ts device. e) Short circuit current output as a function of different concentrations of ZnO-Ts-doped PVDF composite films. f) Output voltage obtained from 4% ZnO-Ts device at different frequencies.

mance as it is driven by surface charges and it is in good agreement with literature.[36]

3.2. Discussion of Piezoelectric Properties

The piezoelectric properties of PVDF are closely tied to its crystalline phases, particularly the β-phase, which is known for its high piezoelectric activity due to the alignment of molecular dipoles. The processing conditions used in this study are consistent with those known to promote the formation of the β-phase in PVDF.[37] Based on these prior studies,[38] it is reasonable to infer that the β-phase is predominant in our PVDF films, contributing to the observed piezoelectric performance.[39] The inclusion of ZnO tetrapods in the composite films further enhances piezoelectricity, likely due to their unique tetrapodal structure, which has been shown to improve mechanical stress distribution and augment the overall piezoelectric response.[40] This observation is in good agreement with literature precedences that have demonstrated that 3DZnO tetrapods can significantly boost the piezoelectric properties when incorporated into polymer matrices.[24]

The observed piezoelectric output voltage of the bare PVDF aligns well with the expected performance of β-phase PVDF films.[41] The enhanced piezoelectric response can be attributed to mechanisms well-documented in the literature, wherein the β-phase of PVDF and the unique structure of ZnO tetrapods play pivotal roles.[42] Our findings suggest that the processing conditions likely facilitated the formation of the β-phase in PVDF, while the zinc oxide

© 2025 The Author(s). Small published by Wiley-VCH GmbH

16136829, 0, Downloaded from https://onlinelibrary.wiley.com/doi/10.1002/smll.202408414 by Zaffar Shaikh - Benazir Bhutto Shaheed , Wiley Online Library on [15/04/2025]. See the Terms and Conditions (https://onlinelibrary.wiley.com/terms-and-conditions) on Wiley Online Library for rules of use; OA articles are governed by the applicable Creative Commons License

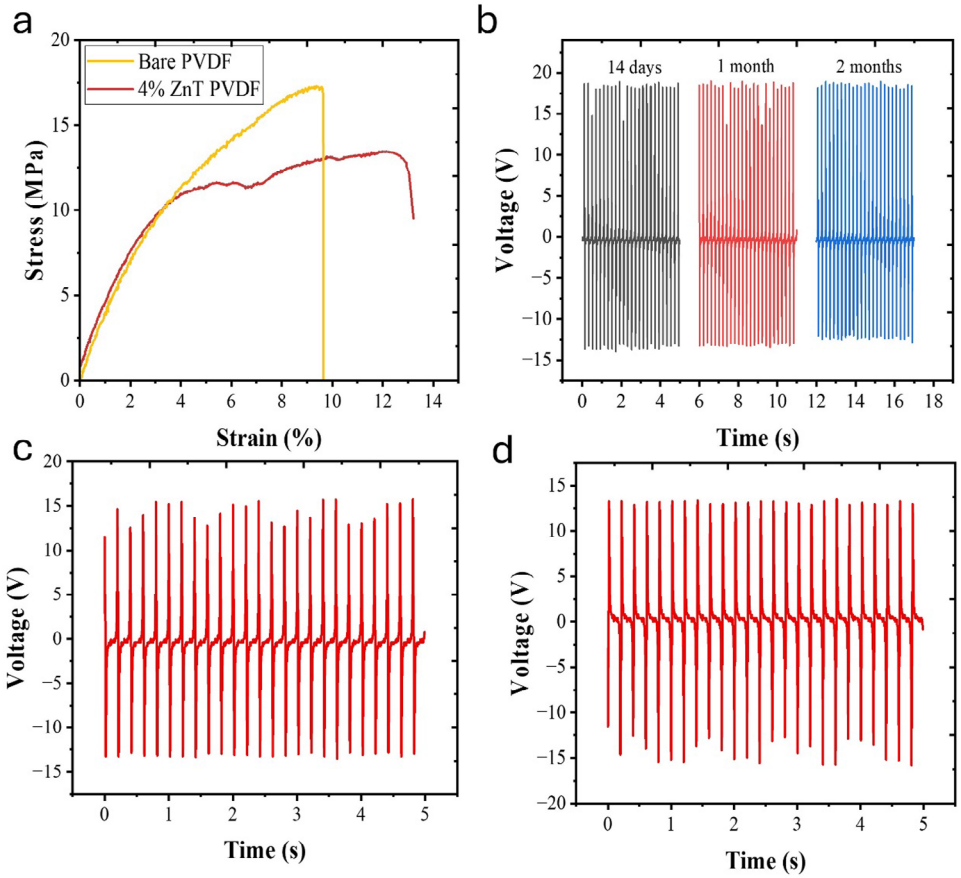

Figure 4. The stress-strain curve illustrates the mechanical behavior of the 4% ZnO tetrapod-PVDF film in comparison with pristine PVDF films. The Young's modulus of 3.60 MPa indicating its relative flexibility whereas the bare PVDF material gives a modulus of 12.78 MPa. The photograph embedded shows the stretching, bending, and twisting of these composite films. b) Device stability test showing open circuit voltage stable after 1 month without any considerable change. c) Switching polarity test gives an open-circuit output voltage of PENG with 4 wt.% of ZnO tetrapod in PVDF with Forward connection d) Reverse connection.

tetrapods contributed significantly to the overall piezoelectric effect.[31].

3.3. Intrinsic Mechanism of Piezoelectricity in ZnO Tetrapods

ZnO tetrapods are known for their inherent piezoelectricity due to their non-centrosymmetric wurtzite structure.[24] When embedded in a piezoelectric polymer, the high dielectric constant of ZnO can enhance the alignment of dipoles in the polymer matrix during poling.[43] This improved alignment leads to stronger polarization and higher piezoelectric coefficients in the composite. These are also active fillers that contribute to the overall piezoelectric output by generating an electric charge when subjected to mechanical deformation.[23] Effective load transfer enhances the deformation-induced charge generation in the ZnO, which contributes to the composite's overall piezoelectric performance. ZnO tetrapods can act as charge traps and facilitate the redistribution of charges within the composite.[44] Their unique tetrapodal structure provides a multidirectional response and enhances the overall electromechanical properties of the composite, making it suitable for high-performance piezoelectric applications.[30]

3.4. PENG Energy Harvesting Studies

The PENG studies of Zn-T doped PVDF samples reveal the energy harvesting potential of composite films. The packaged device with electrodes and the PDMS is depicted in the above **Figure 3a**. The electrical connections were made by copper wires to make a complete PENG device. The scheme shows the working principle of PENG. When external force is applied, it leads to a change in symmetry of charges which in turn leads to consequent flow of electrons to the external circuit. In summary, the output voltage is just a reflection of the external force applied to the PENG device. This forms the foundation of PENG based sensors. The composite films can be bent to any angle and hence are very sensitive to any physical deformation. We used a linear motor to apply a mechanical force, following which a potential is generated between the two electrodes in the PENG device, as evidenced by generation of positive and negative potentials. When an external load is available, the electrons flow through this path and are measured via an electrometer. The complete stoppage of electrons occurs when the applied force is released as a result piezoelectric potential vanishes and electrons flow in opposite directions (Figure 3b).

© 2025 The Author(s). Small published by Wiley-VCH GmbH

16136829, 0, Downloaded from https://onlinelibrary.wiley.com/doi/10.1002/smll.202408414 by Zaffar Shaikh - Benazir Bhutto Shaheed , Wiley Online Library on [15/04/2025]. See the Terms and Conditions (https://onlinelibrary.wiley.com/terms-and-conditions) on Wiley Online Library for rules of use; OA articles are governed by the applicable Creative Commons License

Table 1. Comparison with previously reported zinc oxide-based piezoelectric nanogenerator.

Various works reported on PENG	Fabrication technique	Reported voltages	Refs.
Flexible Pressure Sensor Based on Tetrapod-Shaped ZnO-PDMS	Spin coating	0.4 V	[47]
PVDF–ZnO seeds composite fibers membranes	Electrospinning	1.12 V	[48]
PVDF/ZnO (15 wt.%)/CNT	Solution casting	1.32 V	[49]
Electrospun PVDF-HFP/Co-ZnO Nanofibers	Electrospinning	2.8 V	[50]
PVDF–20% ZnO nanorods	Electrospinning	3.6 V	[51]
ZnO (nanoflower)/PVDF/PDMS	Solution casting	3.16 V	[52]
Zinc oxide Nanoflower-PDMS	Solution casting	4.2 V	[53]
Piezoelectric properties of zinc oxide/iron oxide filled PVDF fibers	Electrospinning	5.9 V	[54]
ZnO nanorods in PVDF matrix	Solution casting	14.6 V	[46]
ZnO NWs @chopped short carbon fiber (CF)/PVDF composite piezoelectric film	Drop casting followed by annealing	14.9 V	[55]
Flexible ZnO microrods/PVDF composite films	Casting followed by phase inversion	15.2 V	[56]
PVDF-MWCNT (0.1 wt.%)-ZnO (15 wt.%)	Drop casting followed by annealing	22 V	[57]
Zinc oxide Tetrapods (4 wt.%)/PVDF composite films	Solution casting	19 V	This work

Initially, we optimized the concentration of ZnOtetrapodsby varying it from 0.5% to 6%. The PENGs were fabricated using the scheme shown above and subjected to interactions with a linear motor operating at at 4Hz. The open-circuit output voltage/short-circuit current of the PENGs exhibited an increase from 4V/0.3 to ≈20V/ 2μA with an increase in ZnO tetrapod intake up to 4 wt.% (Figure 3c,e). However, the output characteristics decreased substantially to 14V/1.5 μA with increased tetrapod concentration at 6% wt. The enhancement in output characteristics with increased tetrapod concentration correlates with the higher concentration of piezoelectric ZnO in the PVDF matrix. The 4% ZnO- tetrapod device when compared with pristine PVDF shows 450% increase in output voltage which can be used in real-time energy harvesting applications (Figure 3d). The possible explanation for increased piezo response with an increase in small ZnO tetrapod concentration is due to a change in the number of attractive atomic interactions between PVDF-ZnO.[44] The decline in output performance beyond 4 wt.% is attributed to Maxwell–Wagner

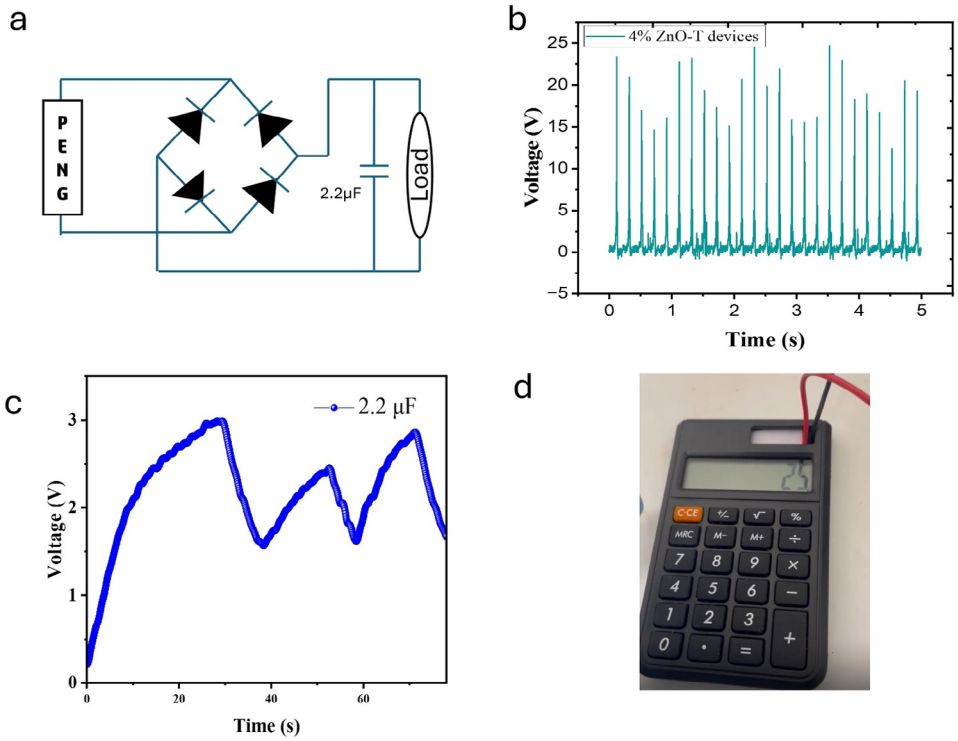

Figure 5. Waveform of electrical responses from self-powered nanofibrous PENG. a) The circuit diagram for connecting PENG with a bridge rectifier and with 2.2 μF capacitor. b) The rectifying voltage with 4% ZnO- tetrapod devices. c) The capacitor charging and discharging of the PENG device. d) Photograph of self-powered calculator driven by the PENG device.

© 2025 The Author(s). Small published by Wiley-VCH GmbH

16136829, 0, Downloaded from https://onlinelibrary.wiley.com/doi/10.1002/smll.202408414 by Zaffar Shaikh - Benazir Bhutto Shaheed , Wiley Online Library on [15/04/2025]. See the Terms and Conditions (https://onlinelibrary.wiley.com/terms-and-conditions) on Wiley Online Library for rules of use; OA articles are governed by the applicable Creative Commons License

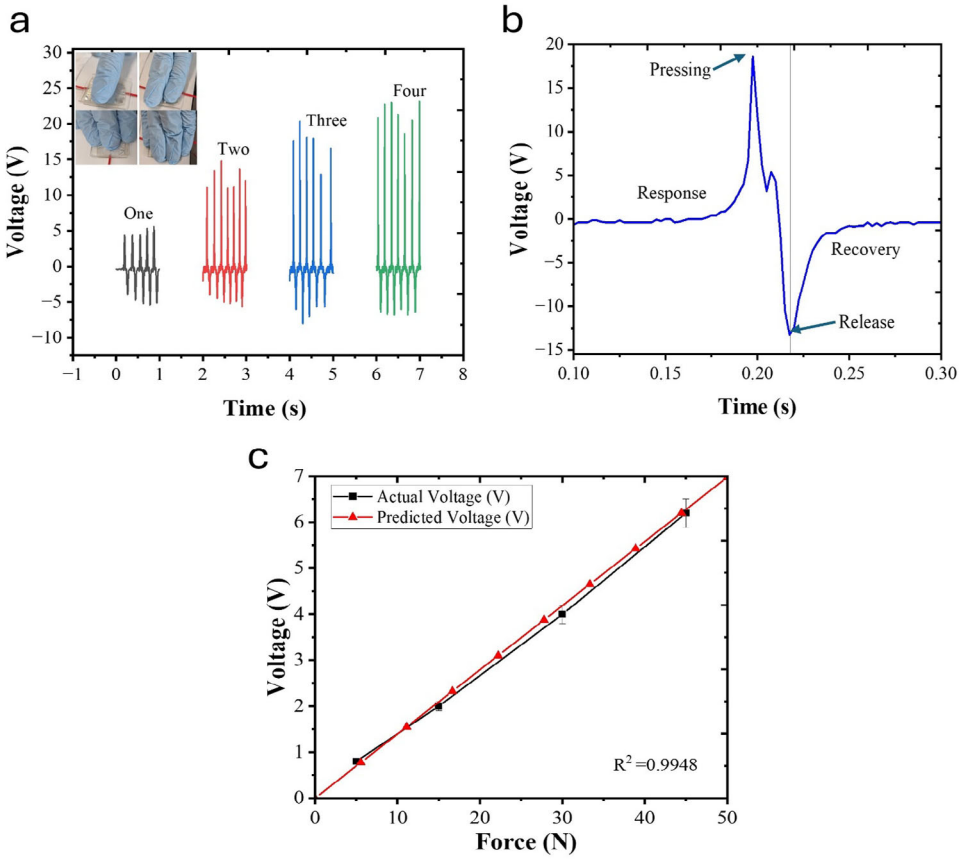

Figure 6. Motion detection and pressure sensing via PENG based on a) finger pressing to detect varied responses with a number of fingers. b) The response recorded of the PENG device was 20ms and the recovery time was 30ms. c) The calibration curve of the piezoelectric nanogenerator via force sensor.

interfacial polarization due to the presence of PVDF and ZnO as two different phases in the composite.[43] The higher concentration of ZnO tetrapods within the polymer matrix leads to an increased number of interfaces with PVDF matrix, promoting Maxwell–Wagner interfacial polarization, consequently enhancing the overall dielectric constant of the composite.[45] Another reason for decreased output voltage with increased concentration can be due to the agglomeration of tetrapods reflected in the SEM studies. The output voltage on the 4% wt. PENG device was tested under different frequencies (2 Hz, 3 Hz, 4 Hz, 5 Hz, 6 Hz). Under fixed frequency of 5Hz gave the highest output voltage of 17V (Figure 3f). The frequency-based voltage output showed a decrease in output voltage after 5Hz due to a reduction of dipolar contribution at high frequency. The results given by the 4 wt.% device show the best energy harvesting results and have been used for further applications in this work. The mechanical behavior of 4% ZnO tetrapod composite film was calculated and gave a Young's modulus of 3.60 MPa and stretched up to 12.94% of its original length before it broke even (**Figure 4**). The initial linear portion represents the elastic deformation, while the subsequent curve shows plastic deformation up to the failure point. The modulus of both the bare and 4% ZnO tetrapod films show that the inclusion of the tetrapods in the matrix enhances the flexibility and toughness and pushes the films into the plastic region rather than snapping at the front. The photograph inset shows that the films can be bent to any angle, demonstrating optimum flexibility and toughness. As demonstrated in Figure 4b, the output characteristics of the fabricated PENG were evaluated over again after 1 month. The results indicated that there was no significant change in the output characteristics. These robust properties make the films suitable for capturing physical interactions of different kinds. such as. Additionally, a switching polarity test was conducted on a PENG fabricated with 4 wt.% ZnO tetrapods in PVDF composite film. The results, illustrated in Figure 4c show that reversing the connection yielded outputs with identical amplitudes but opposite signs. This confirms that the output is attributable to the piezoelectric effect rather than any instrumental artifacts or triboelectric contributions.[46] The comparison table shown below outlines the fabricated PENG device produces remarkably high performance with an optimal quantity of ZnOtetrapods (**Table 1**).

3.5. Energy Harvesting Applications

The circuit diagram for the connection of PENG device to drive a portable calculator by charging a capacitor is shown below (**Figure 5a**). The output voltage of PENG was rectified using a bridge rectifier to charge the capacitor. Here, the rectified voltage of ≈22 V was obtained from the proposed PENG device

© 2025 The Author(s). Small published by Wiley-VCH GmbH

16136829, 0, Downloaded from https://onlinelibrary.wiley.com/doi/10.1002/smll.202408414 by Zaffar Shaikh - Benazir Bhutto Shaheed , Wiley Online Library on [15/04/2025]. See the Terms and Conditions (https://onlinelibrary.wiley.com/terms-and-conditions) on Wiley Online Library for rules of use; OA articles are governed by the applicable Creative Commons License

(Figure 5b). The ZnO tetrapod loaded PENG device was suitable to charge a capacitor of 2.2 μF. It was observed that the device can easily charge the capacitor to drive low-power consuming electronic devices. The charging and discharging curve of 2.2μF (Figure 5c) can easily charge the capacitor up to 3V in 25 s. The image of calculator being directly driven by this PENG device is shown in Figure 5d. A live recording of self-powered calculation via PENG deice is also shown in Supplementary Video S1 (Supporting Information).

3.6. Piezoelectric Sensing Applications

In the previous sections, it was observed that the fabricated PENG with 4% wt. ZnO-tetrapod:PVDF showed the best output characteristics. Such piezoelectric devices are suitable for applications in tactile and force sensing. The piezoelectric composites have been a relatively new technology. It can serve as haptic sensor technology, where energy would be harvested from simple body movements and sensations.[58] The ability to simultaneously detect static and dynamic responses is crucial for effective human motion detection and recognition.[46] Human motion can bring about energy from mechanical stimuli.[59] We used it to measure output generated from finger tapping that generated different voltage responses to matchr single to multi finger interactions (**Figure 6a**). Each finger pressed upon the device gives a typical voltage response for that particular load on the PENG device. As the number of fingers pressed on the device is increased, the output voltage also scales high. This confirms that surface area is also a parameter that can contribute to the voltage readings. The waveforms are observed for their signal duration, intensity, and pattern. Typical waveform responses generated upon pressure are shown in Figure 6b, which carried out a fast response time of 20 ms and an average recovery time of 30 ms. The PENG exhibits excellent stability and sensitivity, accurately reflecting both the frequency and magnitude of external stimuli. In Figure 6c, the calibration curve with a 1kg load cell shows a linear relationship between force applied and voltage generated. The output voltage is directly proportional to the force applied. The speed of the load cell for this calibration was 280mm s^{-1} while the surface area of the probe was 1cm^2 (Video S2, Supporting Information). The previous experiments had a surface area of 6 cm^2 with speed of 0.4 m s^{-1}. A larger surface area allows higher cumulative dipole alignment, leading to a more substantial voltage output. This increased surface engagement enhances the device's overall sensitivity, enabling more efficient conversion of mechanical stress into electrical energy. At higher speeds, the mechanical deformation of the PENG is more rapid, increasing the rate of dipole alignment within the piezoelectric material. The sensitivity of the device is 0.13 V/N considering the surface area and the speed of the load cell as a crucial parameter. Thus this device shows exceptional sensitivity in low-pressure ranges allowing it to detect even the slightest deformations. In summary, tactile sensing can be effectively achieved by using the proposed PENG.

4. Conclusion

The ZnOtetrapod: PVDF piezoelectric nanogenerator (PENG) reported is robust, biocompatible, and multifunctional, capable of independently and simultaneously detecting external stimuli such as pressure under different conditions of mechanical loading, movements, and touch. It benefits from a simple yet very efficient fabrication process, critical for rapid prototyping and integration for capturing human-machine interactions of physical nature. Coupled with quick responsiveness, mechanical flexibility and durability, it is suitable for a wide range of application domains. These applications include real-time, continuious monitoring for long-term data capture, with high-precision, and reliable monitoring of human physical performance as well as applications in elderly age care and health management. Integration of such sensors in bionic devices is higly topical and it is suited to benefit people with bionic limbs or experiencing plantar issues. The combination of versatility and robustness highlights its potential in advanced wearable electronics, soft robotics, movement neuroscience and biomedical devices.

Supporting Information

Supporting Information is available from the Wiley Online Library or from the author.

Acknowledgements

AKP acknowledges funding support from Bionics Queensland 2020 Innovation Award and Australian Defence Science and Technology Group (DSTG) grant on Optomechanics and Acoustic Sensing. YKM acknowledges funding from ESSlighthouse on hard materials in 3D, SOLID(Danish Agency for Science and Higher Education, grant number 8144-00002B) NANOCHEM, BHJ Fonden, and Fabrikant Mads Clausen Fonden, Denmark.

Open access publishing facilitated by Queensland University of Technology, as part of the Wiley - Queensland University of Technology agreement via the Council of Australian University Librarians.

Conflict of Interest

The authors declare no conflict of interest.

Data Availability Statement

The data that support the findings of this study are available from the corresponding author upon reasonable request.

Keywords

3D piezoelectric, force detection, tactile sensor, tetrapods, ZnO

Received: September 16, 2024
Revised: February 4, 2025
Published online:

[1] R. Vinuesa, H. Azizpour, I. Leite, M. Balaam, V. Dignum, S. Domisch, A. Felländer, S. D. Langhans, M. Tegmark, F. Fuso Nerini, *Nat. Commun.* **2020**, *11*, 233.
[2] M. Y. Chougale, M. U. Khan, J. Kim, J. Cosgrove, R. A. Shaukat, Q. M. Saqib, M. Banjade, S. R. Patil, C. Brown, D. Dubal, J. Bae, *Nano Energy* **2023**, *111*, 108399.

© 2025 The Author(s). Small published by Wiley-VCH GmbH

16136829, 0, Downloaded from https://onlinelibrary.wiley.com/doi/10.1002/smll.202408414 by Zaffar Shaikh - Benazir Bhutto Shaheed , Wiley Online Library on [15/04/2025]. See the Terms and Conditions (https://onlinelibrary.wiley.com/terms-and-conditions) on Wiley Online Library for rules of use; OA articles are governed by the applicable Creative Commons License

[3] F. Yin, H. Niu, E.-S. Kim, Y. K. Shin, Y. Li, N.-Y. Kim, *InfoMat* **2023**, *5*, e12424.
[4] T. Shimura, S. Sato, P. Zalar, N. Matsuhisa, *Adv. Electron. Mater.* **2023**, *9*, 2200512.
[5] Y.-C. Lai, S. Ginnaram, S.-P. Lin, F.-C. Hsu, T.-C. Lu, M.-H. Lu, *Adv. Funct. Mater.* **2024**, *34*, 2312443.
[6] Q. He, J. Briscoe, *ACS Appl. Mater. Interfaces* **2024**, *16*, 29491.
[7] a) S.-Y. Yang, V. Sencadas, S. S. You, N. Z.-X. Jia, S. S. Srinivasan, H.-W. Huang, A. E. Ahmed, J. Y. Liang, G. Traverso, *Adv. Funct. Mater.* **2021**, *31*, 2009289. b) H. Guo, J. Wan, H. Wu, H. Wang, L. Miao, Y. Song, H. Chen, M. Han, H. Zhang, *ACS Appl. Mater. Interfaces* **2020**, *12*, 22357.
[8] Q. Zheng, Q. Tang, Z. L. Wang, Z. Li, *Nat. Rev. Cardiol.* **2021**, *18*, 7.
[9] W. Lin, B. Wang, G. Peng, Y. Shan, H. Hu, Z. Yang, *Adv. Sci.* **2021**, *8*, 2002817.
[10] B. Chen, Y. Yang, Z. L. S. W. E. T. N Wang, *Adv. Energy Mater.* **2018**, *8*, 1702649.
[11] Z.-H. Lin, G. Cheng, S. Lee, K. C. Pradel, Z. L. Wang, *Adv. Mater.* **2014**, *26*, 4690.
[12] Z.-Q. Lu, L. Zhao, H.-L. Fu, E. Yeatman, H. Ding, L.-Q. Chen, *Nat. Commun.* **2024**, *15*, 6513.
[13] K. Dong, X. Peng, Z. L. Wang, *Adv. Mater.* **2020**, *32*, 1902549.
[14] S. Han, Q. Zeng, Y. Liang, Q. Xiao, Y. Chen, F. Yan, Y. Xiong, J. Yue, X. Tian, *Adv. Mater. Technol.* **2024**, *9*, 2302172.
[15] L. Algieri, M. T. Todaro, F. Guido, V. Mastronardi, D. Desmaële, A. Qualtieri, C. Giannini, T. Sibillano, M. De Vittorio, *ACS Appl. Energy Mater.* **2018**, *1*, 5203.
[16] X. Huang, Q. Qin, X. Wang, H. Xiang, J. Zheng, Y. Lu, C. Lv, K. Wu, L. Yan, N. Wang, C. Xia, Z. L. Wang, *ACS Nano* **2021**, *15*, 19783.
[17] D. Olmos, G. González-Gaitano, A. L. Kholkin, J. González-Benito, *Ferroelectrics* **2013**, *447*, 9.
[18] S. Baloda, N. Gupta, S. Singh, *IEEE Trans. Electron Devices* **2022**, *69*, 7011.
[19] S. Cherumannil Karumuthil, K. Singh, U. Valiyaneerilakkal, J. Akhtar, S. Varghese, *Sens. Actuators, A* **2020**, *303*, 111677.
[20] G. Chang, X. Pan, Y. Hao, W. Du, S. Wang, Y. Zhou, J. Yang, Y. He, *RSC Adv.* **2024**, *14*, 11775.
[21] L. Vayssieres, *Adv. Mater.* **2003**, *15*, 46.
[22] L. Yan, A. Uddin, H. Wang, *Nanomater. Nanotechnol.* **2015**, *5*, 19.
[23] Z. Moarref, N. H. Fahim, M. Montazer, *Nanotechnology in Electronics*, Wiley, Hoboken, New Jersey **2023**, pp 63–95.
[24] Y. K. Mishra, R. Adelung, *Mater. Today* **2018**, *21*, 631.
[25] F. R. Fan, W. Tang, Z. L. Wang, *Adv. Mater.* **2016**, *28*, 4283.
[26] Z. L. Wang, *Adv. Funct. Mater.* **2008**, *18*, 3553.
[27] G. Nagaraju, Y. H. Ko, J. S. Yu, *Mater. Chem. Phys.* **2015**, *149–150*, 393.
[28] S. Shree, M. Schulz-Senft, N. H. Alsleben, Y. K. Mishra, A. Staubitz, R. L Adelung, *ACS Appl. Mater. Interfaces* **2017**, *9*, 38000.
[29] B. Yin, Y. Qiu, H. Zhang, J. Lei, Y. Chang, J. Ji, Y. Luo, Y. Zhao, L. Hu, *RSC Adv.* **2015**, *5*, 11469.
[30] Z. Zhang, Y. Nan, Y. K. Mishra, M. Willatzen, Z. L. Wang, *Appl. Phys. Lett.* **2023**, *123*, 023501.
[31] Z. Zhang, M. Willatzen, Y. K. Mishra, Z. L. Wang, *Mater. Today Electron.* **2024**, *8*, 100102.
[32] H. Yuan, T. Lei, Y. Qin, R. Yang, *Nano Energy* **2019**, *59*, 84.
[33] S. Mohammadpourfazeli, S. Arash, A. Ansari, S. Yang, K. Mallick, R. Bagherzadeh, *RSC Adv.* **2022**, *13*, 370.
[34] Y. K. Mishra, S. Kaps, A. Schuchardt, I. Paulowicz, Jin, D. Gedamu, S. Freitag, M. Claus, S. Wille, A. Kovalev, S. N. Gorb, R. Adelung, *Part. Part. Syst. Charact.* **2013**, *30*, 775.
[35] Y. K. Mishra, G. Modi, V. Cretu, V. Postica, O. Lupan, T. Reimer, I. Paulowicz, V. Hrkac, W. Benecke, L. Kienle, R. Adelung, *ACS Appl. Mater. Interfaces* **2015**, *7*, 1430.
[36] Z. Jiang, Z. Xiao, Z. Tao, X. Zhang, S. Lin, *RSC Adv.* **2021**, *11*, 26534.
[37] M. Yasar, P. Hassett, N. Murphy, A. Ivankovic, *ACS Omega* **2024**, *9*, 26020.
[38] W. Ma, J. Zhang, S. Chen, X. Wang, *Appl. Surf. Sci.* **2008**, *254*, 5635.
[39] F. Lederle, C. Härter, S. Beuermann, *J. Fluorine Chem.* **2020**, *234*, 109522.
[40] I. Paulowicz, V. Postica, O. Lupan, N. Wolff, S. Shree, A. Cojocaru, M. Deng, Y. K. Mishra, I. Tiginyanu, L. Kienle, R. Adelung, *Sens. Actuators, B* **2018**, *262*, 425.
[41] R. S. Kumar, T. Sarathi, K. K. Venkataraman, A. Bhattacharyya, *Mater. Lett.* **2019**, *255*, 126515.
[42] S. D. Mahapatra, P. C. Mohapatra, A. I. Aria, G. Christie, Y. K. Mishra, S. Hofmann, V. K. Thakur, *Adv. Sci.* **2021**, *8*, 2100864.
[43] X. Zhang, M.-Q. Le, O. Zahhaf, J.-F. Capsal, P.-J. Cottinet, L. Petit, *Mater. Des.* **2020**, *192*, 108783.
[44] J. M. Marmolejo-Tejada, L. De, J. Roche-Yepes, C. A. Pérez-López, J. A. P. Taborda, A. Ávila, A. Jaramillo-Botero, *J. Chem. Inf. Model.* **2021**, *61*, 4537.
[45] A. Mahapatra, R. S. Ajimsha, D. Deepak, P. Misra, *Sci. Rep.* **2024**, *14*, 11871.
[46] A. Mahapatra, R. S. Ajimsha, M. O. Ittoop, A. Sharma, S. Karmakar, A. Shaikh, P. R. Sankar, P. Misra, *J. Alloys Compd.* **2023**, *960*, 170898.
[47] Y. Liu, G. Lu, L. Guo, Y. Zhang, M. Chen, *IEEE Sens. J.* **2023**, *23*, 3532.
[48] B. Sun, X. Li, R. Zhao, H. Ji, J. Qiu, N. Zhang, D. He, C. Wang, *J. Mater. Sci.* **2019**, *54*, 2754.
[49] A. Kumar, S. Jaiswal, R. Joshi, S. Yadav, A. Dubey, D. Sharma, D. Lahiri, I. Lahiri, *Polym. Compos.* **2023**, *44*, 4746.
[50] H. Parangusan, D. Ponnamma, M. A. A. Al-Maadeed, *Sci. Rep.* **2018**, *8*, 754.
[51] R. S. Sabry, A. D. Hussein, *Mater. Res. Express* **2019**, *6*, 105549.
[52] H. Khatun, D. Pamu, S. P. Balmuchu, N. S. Singh, U. Sarma, *Sens. Actuators, A* **2023**, *364*, 114812.
[53] K. Jeronimo, V. Koutsos, R. Cheung, E. Mastropaolo, *Sensors* **2021**, *21*, 5873.
[54] A. M. AlAhzm, M. O. Alejli, D. Ponnamma, Y. Elgawady, M. A. A. Al-Maadeed, *J. Mater. Sci.: Mater. Electron.* **2021**, *32*, 14610.
[55] Y. Li, J. Sun, P. Li, X. Li, J. Tan, H. Zhang, T. Li, J. Liang, Y. Zhou, Z. Hai, J. Zhang, *J. Mater. Chem. A* **2023**, *11*, 13708.
[56] D. P. Ojha, B. Joshi, E. Samuel, A. Khadka, A. Aldalbahi, G. Periyasami, D. Choi, S. An, S. S. Yoon, *Int. J. Energy Res.* **2023**, *2023*, 3074782.
[57] S. Pratihar, A. Patra, A. Sasmal, S. K. Medda, S. Sen, *Soft Matter* **2021**, *17*, 8483.
[58] Y. Wang, Y. Yu, X. Wei, F. Narita, *Adv. Mater. Technol.* **2022**, *7*, 2200318.
[59] R. Riemer, A. Shapiro, *J. NeuroEng. Rehabil.* **2011**, *8*, 22.

© 2025 The Author(s). Small published by Wiley-VCH GmbH

16136829, 0, Downloaded from https://onlinelibrary.wiley.com/doi/10.1002/smll.202408414 by Zaffar Shaikh - Benazir Bhutto Shaheed , Wiley Online Library on [15/04/2025]. See the Terms and Conditions (https://onlinelibrary.wiley.com/terms-and-conditions) on Wiley Online Library for rules of use; OA articles are governed by the applicable Creative Commons License